Journal of Physical Science, Vol. 35(3), 17–25, 2024

Preparation and Characterisation of CdO@Au Nanoparticles by Hybrid System Using Laser Ablation and Plasma Jet Methods for Cytotoxicity Against Rat Embryonic Fibroblast Cell Line

Noha H. Harb, Haider Y. Hammod, Sara T. Mohmmed and Ban H. Adil*

Department of Physics, College of Science for Women, University of Baghdad, 10071 Baghdad, Iraq

*Corresponding author: banha_phys@csw.uobaghdad.edu.iq

Published online: 30 November 2024

To cite this article: Harb, N. H. et al. (2024). Preparation and characterisation of CdO@Au nanoparticles by hybrid system using laser ablation and plasma jet methods for cytotoxicity against rat embryonic fibroblast cell line. *J. Phys. Sci.*, 35(3), 17–25. https://doi.org/10.21315/jps2024.35.3.2

To link this article: https://doi.org/10.21315/jps2024.35.3.2

ABSTRACT: *The purpose of the research is to see if cadmium oxide@gold (CdO@Au) nanoparticles produced using the laser ablation and plasma jet method in deionised water (DW) solution could be a viable alternative to typical materials in cytotoxicity of rat embryonic fibroblast (REF) normal cell line. The cadmium nanoparticle core was prepared using a Q-switched Nd:YAG laser at a wavelength of 1,064 nm, with laser pulse energies varying between 800 mJ and 1,000 mJ over 500 shots. Gold nanoparticles shell prepared using atmospheric pressure plasma jet. The structural analysis process used X-ray diffraction (XRD) and UV-Vis absorption spectroscopy to study the surface plasmon resonance (SPR) to follow the fast changes in the nanoparticles (NPs) colloidal solutions brought on by the interaction between Au sheets and CdO core. From UV-Vis transmittance and absorbance spectra, it was observed that the transmittance pattern that can be obtained decreases. At the same time, the energy gap increases with the increase of laser energy, and this may be due to the increase in absorption. The XRD investigation revealed that the polycrystalline structure of CdO@Au NPs and their preferred orientation along (111) direction. The normal REF cell line was employed in the study to investigate the cytotoxicity of CdO@Au nanoparticles. After 48 h of exposure, the CdO@Au NPs displayed the maximum toxicity at a concentration of 100%.*

Keywords: CdO@Au NPs, Nd:YAG laser, plasma Jet, cytotoxicity assay, REF cells line

1. INTRODUCTION

Cadmium oxide (CdO) is a semiconductor of the n-type with a large energy band gap 2.2 eV–3.3 eV, an ionic nature, and excellent transmittance in the solar spectrum's visible region. One of the most well-known applications of CdO nanoparticles (NPs) is in optoelectronics, which also includes gas sensors, solar cells and phototransistors.[1–3] Cancer cell eradication and tailored medicine delivery have now become possible thanks to CdO NPs.[4,5] Against some harmful microorganisms that are resistant to antibiotics, CdO NPs have outstanding antibacterial activity.[6,7] Gold (Au) nanoparticles have prospective uses due to their distinctive mechanical, chemical, electrical, optical and thermal properties compared to bulk gold.[8,9] At the macro scale, bulk gold thought to be biologically inert, Due to its surface plasmon resonance excitation qualities, gold shows a diversity of behaviours at the nanoscale.[10,11] Typically, nanoparticles used in biotechnology typically range in size from 10 nm–500 nm, seldom exceeding 700 nm. These particles' nanoscale permits a range of communications with biomolecules on the cell surfaces and within the cells in a way that can be decoded and attributed to different biochemical and physiochemical characteristics in these cells. Due of the high plasmon resonance they are connected with, noble metal nanoparticles like Au and silver (Ag) have attracted a lot of attention.[12,13] Metal nanoparticles' surface plasmon resonance differs from that of bulk materials and is greatly influenced on the shape, dimension, degree of aggregation of the nanoparticles and as well as the electrical and dielectric characteristics of media in which they are dispersed.[14,15] A biphasic material of the core/shell type has an inner core structure and an exterior shell formed of various materials. These particles have attracted attention because they can display special qualities due to the interaction between the materials used for the core and shell, as well as their geometry and construction. In addition, it was developed in a way that the thin, more expensive shell material can be carried by a core material that is more reactive, thermally stable or oxidatively stable.[16] Depending on how the cores and shells interact, CdO@Au NPs (core@shell) may possess properties that work in harmony with one another or provide new properties.[17] The surface chemistry of the core@shell nanoparticles, which boosts their ability to connect with medicines, receptor ligands, etc., makes them primarily intended for biological applications. As a result, new nanoparticles have been created, which work better with biological systems than bulk material. Typically, there are two types of biomedical nanotechnology applications outside and inside body's. While researchers are focusing on targeted medicine delivery, implanting insulin pumps and gene therapy for applications inside the body, the application outside the body uses biosensors and biochips to monitor blood and other biological materials.[18]

This study aimed to synthesise Cd@Au NPs core shell using a hybrid system using laser ablation and plasma jet methods to determine how laser energy pulses affect the discrete independence in terms of optical and synthetic gain, as well as calculate the cytotoxicity of normal cells line (rat embryonic fibroblast [REF]) in order to use it for future studies of medical applications.

2. EXPERIMENTAL

2.1 Preparation of the CdO NPs

The targets were Cd plates with dimensions of 1 cm × 1 cm and a purity of 99.9%. Before each ablation, the target surface was polished with fine paper and rinsed with ethanol and deionised water (DW) to remove any residue from previous ablation processes. In this study, DW served as the liquid medium. Prepare CdO NPs core suspensions in liquid by pulsed Q-switched Nd: YAG laser system 1,064 nm with pulse energies of 800 mJ, 900 mJ and 1,000 mJ, output pulse durations of 10 ns. The focusing of the 2.4 mm broad laser beams was done using a convex lens has a length of focus of 12 cm. CdO target buried in the bottom of a clear glass jar with 3 mL of DW, to get a volume of the solution equal to 5 mL and the procedure was repeated. After the ablation procedure, the colloidal solution took on a faint tint to show that CdO NPs had formed.

2.2 Preparation of the Au NPs

The molecular weight of the aqueous gold salts, chloroauric acid tetrahydrate ($HAuCI4.4H_2O$) was 411.8 g/mol, and they were dissolved in DW as a concentration of 0.5 mM by using Equation 1 to calculation concentration.

$$\text{Concentration} = \frac{\text{Mass}}{\text{Molecular weight} \times \text{Volume}} \quad (1)$$

2.3 Preparation of the CdO@Au NPs

The total volume of the solution was 10 mL after 5 mL of produced nano-cadmium oxide and 5 mL of $HAuCI_4.4H_2O$ solution were added to it. Synthesise CdO@Au NPs by atmospheric pressure plasma jet by Ar gas 3 L/min, the jet was set 1 mm above the aqueous solution. Plasma jet is produced by holding a 10 cm stainless steel metal tube with internal diameter of 1 mm and connecting it to the cathode of the power supply. It can process power up to 20 kV, and the stainless steel conductive strip ends have a (1×1) flat end that is 7 cm wide and

5 mm thick, as shown in Figure 1. After the two materials were prepared, an amount of five moles was taken from each of them, and they were stirred well. They were exposed to plasma for a period of not less than 10 min. We notice that the colour of the mixture has changed to a violet colour, indicating the formation of particles CdO@Au. An UV-Vis spectrophotometer with a double beam was used for investigating the optical characteristics. Application of Tauc's Equation 2 for direct transition resulted in a graphic estimation of the optical band gap.[3]

$$(\alpha hv) = A\left(hv - E_g\right)^{\frac{1}{2}} \tag{2}$$

Where A is an optical constant. Plotting $(hv)^2$ versus h will allows for the determination of the band gap.

CdO@Au NPs were deposited onto n-type silicon (111) using the drop-casting method. The crystalline structure was examined using X-ray diffraction (XRD) in a continuous scan range of 10°–100°. The toxicity of CdO@Au NPs was determined by testing dilutions at 6.25%, 12.5%, 25%, 50% and 100%.

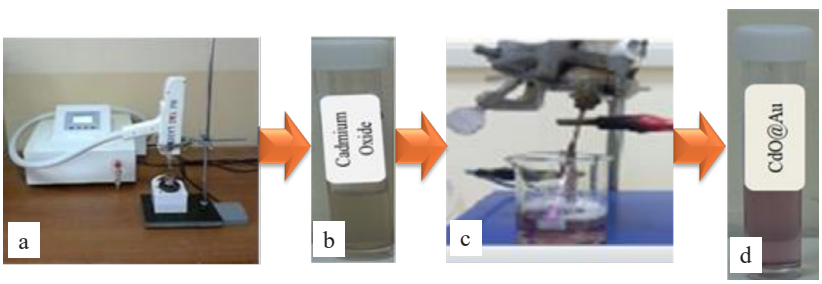

Figure 1: Synthesis of CdO@Au (a) laser ablation scheme, (b) CdO NPs, (c) plasma jet scheme and (d) CdO@Au NPs.

3. RESULTS AND DISCUSSION

Figure 2 shows optical transmission spectra of CdO@Au NPs prepared by 1,064 nm, using UV-Vis spectrum in the region 220 nm–1,200 nm. Laser energy of 800 mJ, 900 mJ and 1,000 mJ used for pulsed laser ablation in liquid. It is a UV-detector because it absorbs light in the UV range. Transmission peak of sample produced at 1,000 mJ had a greater peak than that produced at 800 mJ, which was related to higher concentration of NPs. The transmission pattern of all CdO@Au NPs prepared increases with the increase of wavelength (λ), also can be obtained that the transmission decreases with the increase of laser energy and this may be due to the increase in the absorption.

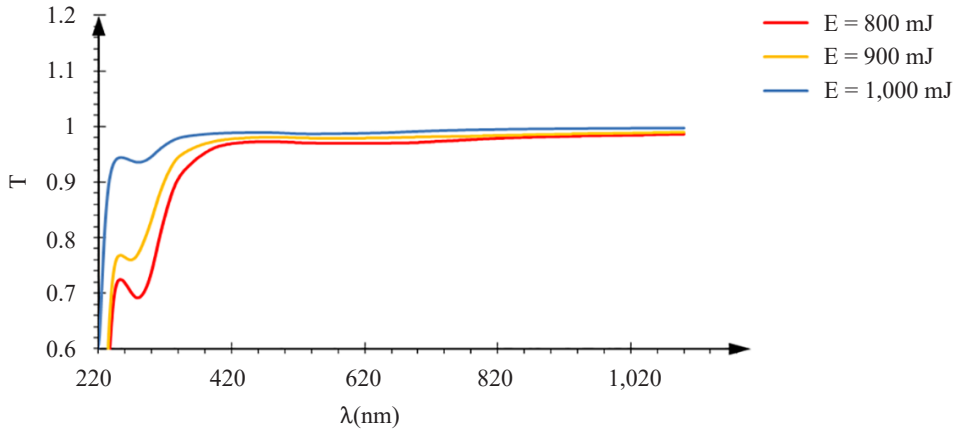

Figure 2: Transition spectra for CdO@Au NPs prepared at 800 mJ, 900 mJ and 1,000 mJ laser energies, with 500 shots by laser ablation-plasma jet method.

For CdO@Au NPs with various laser energy pulses, Figure 3 displays the (αhυ) as a function of *hv*. Tauc equation has been used to calculate the optical energy gap values for CdO@Au NPs. Optical band gap varies from 3.18 eV–3.8 eV with increasing laser energy from 800 mJ–1,000 mJ. This outcome demonstrated that CdO was incorporated with Au and that their energy bands overlapped. As a result of as particle size decreases, the absorption edge shifts to lower wavelengths due to the quantum confinement phenomena. All manufactured samples showed band gaps that were higher than those of bulk CdO.

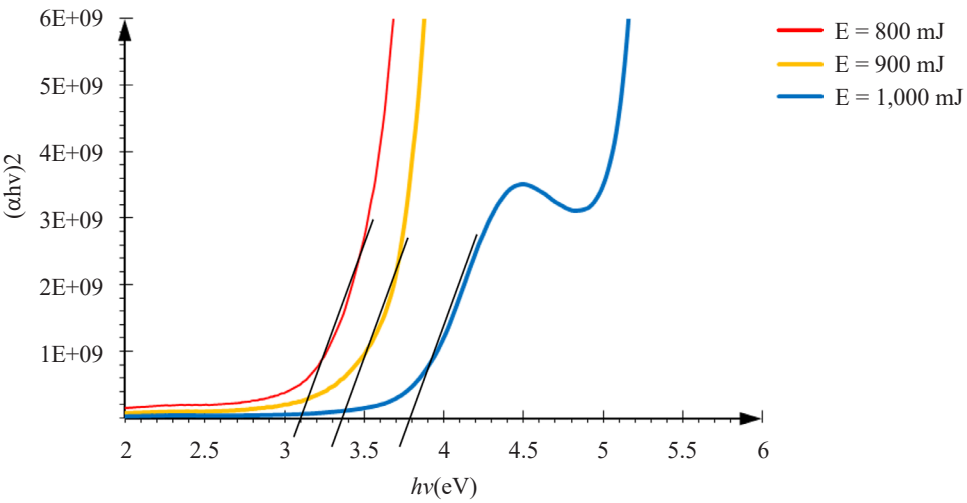

Figure 3: The electron volts (E_g) for CdO@Au NPs prepared at 800 mJ, 900 mJ and 1,000 mJ laser energies, with 500 shots by laser ablation-plasma jet method.

In Figure 4, the XRD structures for CdO@Au NPs drop-cast on a silicon n-type substrate and prepared at 800 mJ, 900 mJ and 1,000 mJ are displayed. The XRD structure exhibit peaks centered at 2θ = 37.9° for Si (002). 2θ = 38.27°, 2θ = 44.59° and 2θ = 66.737° for the Au and which corresponds to (111), (200) and (220) planes. 2θ = 33.040°, 2θ = 38.36° and 2θ = 55.336° for the CdO polycrystalline structure and a cubic phase, which corresponds to (111), (200) and (220) planes. According to Figure 4, as the laser energy increases, the crystalline structure gets more solidified and secondary peaks start to appear. The average crystal size for Au NPs produced at 800 mJ, 900 mJ and 1,000 mJ laser energies determine by the Debye Sherrer formula, were 28 nm, 22 nm and 18 nm, respectively. The crystal size for CdO were 34 nm, 15 nm and 12 nm.[19]

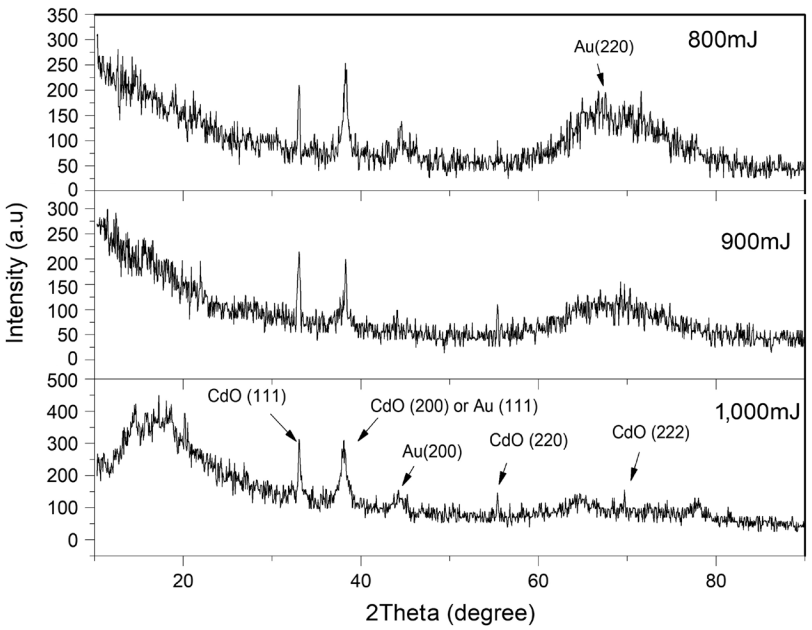

Figure 4: XRD patterns for CdO@Au NPs prepared at 800 mJ, 900 mJ and 1,000 mJ laser energies by laser ablation-plasma jet method.

Our study used the normal cell line (REF) to test the cytotoxicity of CdO@Au nanoparticles different concentrations using a 96-well micro plate. Seeding 10,000 cells were cultured in each well and incubated in the incubator at a temperature of 37°C for 24 h until a monolayer was formed and examined with an inverted microscope cells are exposed with sequential concentrations of the nanomaterial (see Figure 5), a group is left unaffected and is referred to as the control group. The attempts are repeated three times to confirm the validity of the results, and then they are incubated at a temperature of 37°. In addition,

100 µL of diluted methyl thiazolyl tetrazolium (MTT) (diluted using 1 mL of free serum medium) was added (100 µL of MTT dilute for each well) before the mixture was incubated for 2 h. The mixture was then decanted off, and 50 µL of dimethyl sulfoxide (DMSO) was added for each well. The mixture was then re-incubated for 40 min at 37°C. Additionally, the microplate reader has been used to read the results at wavelengths of 584 nm in order to calculate the percentage of normal REF cells (cytotoxcity rate).[20] Following this, the mean value for each group will be estimated. The experimental results where $*P < 0.5$, $**P < 0.1$, $***P < 0.01$ and $****P < 0.001$ are analysed using GraphPad Prism v7.0.

Cytotoxicity is calculated by applying Equation 3:[21]

$$\text{Cytotoxicity} = \frac{\text{Control} - \text{treated}}{\text{Control}} \times 100 \tag{3}$$

We note that the greatest toxicity of Cdo@Au NPs 30% at the nano-concentration of 100% after exposing the cells for 48 h.

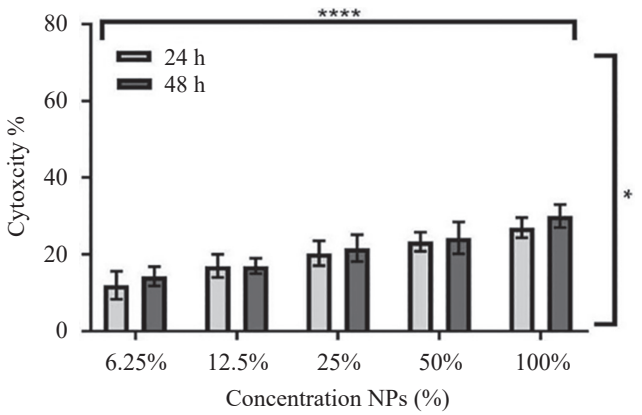

Figure 5: Test the cytotoxicity of CdO@Au nanoparticles.

4. CONCLUSIONS

In this work, laser ablation and plasma jet of pure metal targets were used to successfully produce colloidal metal CdO@Au NPs in DW. It is UV-detector because it absorbs light in the UV range. Because particle sizes are growing, as laser energy increases, the band gap changes toward higher energies. The polycrystalline nature of CdO with cubic type and Au with the cubic structure was revealed by XRD measurements, and transition data showed that the plasmon peak increased with increasing laser power, indicating a rise in NP concentration.

Cdo@Au NPs' greatest toxicity is 30% at the nano-concentration of 100% after exposing the cells for 48 h. Due to their mechanical, optical and thermal capabilities, Cd and Au nanoparticles attracted significant interest in biomedicine. These strong potentials also pose a toxicity concern due to the interactions they have with biological tissues and molecules.

5. ACKNOWLEDGEMENTS

The authors gratefully acknowledge the financial support from University of Baghdad, College of Science for Women, and Biotechnology research center Al-Nahrain University, Baghdad, Iraq. The authors would like to thank Professor Ahmed S Obaid for his advice.

6. REFERENCES

1. Aldwayyan, A. S. et al. (2013). Synthesis and characterization of CdO nanoparticles starting from organometalic dmphen-CdI2 complex. *Int. J. Electrochem. Sci.*, 8(8), 10506–10514. https://doi.org/10.1016/S1452-3981(23)13126-9
2. Heidari, A. & Brown, C. (2015). Study of composition and morphology of cadmium oxide (CdO) nanoparticles for eliminating cancer cells. *J. Nanomed. Res.*, 2(5), 00042. https://doi.org/10.15406/jnmr.2015.02.00042
3. Harb, N. H. (2018). The structure and optical properties of Ag doped CdO thin film prepared by pulse laser deposition (PLD). *Baghdad Sci. J.*, 15(3), 0300. https://doi.org/10.21123/bsj.2018.15.3.0300
4. Zafar, H., Abbasi, B. H. & Zia, M. (2019). Physiological and antioxidative response of Brassica nigra (L.) to ZnO nanoparticles grown in culture media and soil. *Toxicol. Environ. Chem.*, 101(3–6), 281–299. https://doi.org/10.1080/02772248.2019.1691555
5. Zahera, M. et al. (2020). Cadmium oxide nanoparticles: An attractive candidate for novel therapeutic approaches. *Colloids Surf A Physicochem. Eng. Asp.*, 585, 124017. https://doi.org/10.1016/j.colsurfa.2019.124017
6. Abd, A. N., Al Marjani, M. F. & Kadham, Z. A. (2018). Synthesis of CdO NPs for antimicrobial activity. *Int. J. Thin Films Sci. Technol.*, 7(1), 43–47. https://doi.org/10.18576/ijtfst/070106
7. Ghotekar, S. (2019). A review on plant extract mediated biogenic synthesis of CdO nanoparticles and their recent applications. *Asian J. Green Chem.*, 3(2), 187–200. https://doi.org/10.22034/ajgc.2018.140313.1084
8. Mazhir, S. N. et al. (2020). A study of plasma parameters in gold sputtering system by means of optical emission spectroscopy. *IOP Conf. Ser.: Mater. Sci. Eng.*, 871(1), 012081. https://doi.org/10.1088/1757-899X/871/1/012081
9. Bracamonte, M. V. et al. (2011). Quaternized chitosan as support for the assembly of gold nanoparticles and glucose oxidase: Physicochemical characterization of the platform and evaluation of its biocatalytic activity. *Electrochim. Acta*, 56(3), 1316–1322. https://doi.org/10.1016/j.electacta.2010.10.022

10. Aillon, K. L. et al. (2009). Effects of nanomaterial physicochemical properties on in vivo toxicity. *Adv. Drug Deliv. Rev.*, 61(6), 457–466. https://doi.org/10.1016/j.addr.2009.03.010
11. Marsich, E. et al. (2011). Biological response of hydrogels embedding gold nanoparticles. *Colloids Surf. B Biointerfaces*, 83(2), 331–339. https://doi.org/10.1016/j.colsurfb.2010.12.002
12. Mody, V. V., Nounou, M. I. & Bikram, M. (2009). Novel nanomedicine-based MRI contrast agents for gynecological malignancies. *Adv. Drug Deliv. Rev.*, 61(10), 795–807. https://doi.org/10.1016/j.addr.2009.04.020
13. Aktas, B., Tagirov, L. & Mikailov, F. (2004). *Nanostructured magnetic materials and their applications*. Netherlands: Springer Dordrecht. https://doi.org/10.1007/978-1-4020-2200-5
14. Bohren, C. F. & Huffman, D. R. (2008). *Absorption and scattering of light by small particles*. United States: John Wiley & Sons. https://doi.org/10.1002/9783527618156
15. Klabunde, K. J. & Richards, R. M. (2009). *Nanoscale materials in chemistry*. United States: John Wiley & Sons. https://doi.org/10.1002/0471220620
16. Nomoev, A. V. et al. (2015). Structure and mechanism of the formation of core–shell nanoparticles obtained through a one-step gas-phase synthesis by electron beam evaporation. *Beilstein J. Nanotechnol.*, 6(1), 874–880. https://doi.org/10.3762/bjnano.6.89
17. Gawande, M. B. et al. (2015). Core–shell nanoparticles: Synthesis and applications in catalysis and electrocatalysis. *Chem. Soc. Rev.*, 44(21), 7540–7590. https://doi.org/10.1039/C5CS00343A
18. Wei, C. et al. (2007). Nanomedicine and drug delivery. *Med. Clin. N. Am.*, 91(5), 863–870. https://doi.org/10.1016/B978-0-12-820773-4.00006-8
19. Obaid, A. S., Mahdi, M. A. & Hassan, Z. (2012). Nanocoral PbS thin film growth by solid-vapor deposition. *Optoelectron. Adv. Mater. Rapid Commun*, 6(3–4), 422–426.
20. Mohammed, M. S. et al. (2022). Plasma jet prepared gold and silver nanoparticles to induce caspase-independent apoptosis in digestive system cancers. *Mater. Sci. Forum*, 1050, 51–63. https://doi.org/10.4028/www.scientific.net/MSF.1050.51
21. Raheem, M. A. & Adil, B. H. (2023). Thermal effect of laser on silver nanoparticles synthesized by the cold plasma method on cancer cells. *Plasma Med.*, 13(1), 29–38. https://doi.org/10.1615/PlasmaMed.2023047809